

# Carbon nanotube in different shapes

Carbon nanotubes (CNTs) have been well studied theoretically and experimentally. Perfect CNTs have a crystalline structure formed by hexagonal network; defects cause the tubule to curve. CNTs with different tubule morphologies have their own special properties and potential applications. So far, many different shapes, such as straight, waved, coiled, and branched, are predicted, observed, and target synthesized. This article reviews CNTs in different shapes formed during growth, their morphologies and their possible applications.

Mei Zhang\* and Jian Li

High-Performance Materials Institute, Florida State University; Department of Industrial and Manufacturing Engineering, FAMU-FSU College of Engineering, Tallahassee, FL 32310, USA

\*E-mail: [mzhang@eng.fsu.edu](mailto:mzhang@eng.fsu.edu)

Carbon Nanotubes (CNTs) are cylindrical shells made, in concept, by rolling graphene sheets into a seamless cylinder. CNTs exist as either single-wall nanotubes (SWNTs) or multi-walled nanotubes (MWNTs). The SWNT consists of a single graphene sheet, which is a planar array of benzene molecules, involving only hexagonal rings with double and single carbon-carbon bonding. The choice of rolling axis relative to the hexagonal network of the graphene sheet and the radius of the closing cylinder allows for different types of SWNTs, which vary from insulating to conducting<sup>1</sup>. **Figures 1a, 1b, and 1c** show SWNTs of three different types<sup>2</sup>: armchair, zigzag, and chiral. The twist of the chiral nanotube is clearly evident in the lower **Fig. 1c**, a perspective view along the tube axis, and in **Fig. 1d**, a scanning probe microscope (SPM) picture of a chiral SWNT<sup>3</sup>. MWNTs comprise an array of such nanotubes that are concentrically nested. A transmission electron microscope (TEM) image of a nine-walled CNT is shown in **Fig. 1e**. CNTs with perfect crystalline structure are straight cylinders.

Iijima's report<sup>4</sup> in 1991 brought carbon nanotubes into the awareness of the scientific community and triggered a deluge of interest in carbon nanotubes. Shortly after this "rediscovery", CNTs in different shapes (toroidal<sup>5</sup>, coiled<sup>6,7</sup>, and branched<sup>8-10</sup>) other than the straight were predicted theoretically. **Figs. 1f-g** show the illustrations of bent (kink)<sup>11</sup>, branched<sup>12</sup>, and coiled<sup>5</sup> SWNT structures. All these structures are based on the insertion of non-hexagonal defects in seamless hexagonal networks. In particular, the models of the regular helical coils of CNT's are based on a very specific arrangement of pentagons and heptagons in a perfect hexagonal lattice<sup>7,13</sup>. If the regular arrangement is perturbed by misplacing one single non-hexagonal ring, the structure will not be a regular coil any more<sup>13</sup>. The model also shows that the regular helically coiled nanotubes can be built with non-hexagonal/hexagonal ratio higher than unity<sup>14,15</sup>.

Experimentally, CNTs are formed during synthesis. In most cases, CNT grows away from the catalyst particle by the deposition of carbon in the contact region between the particle and the already formed

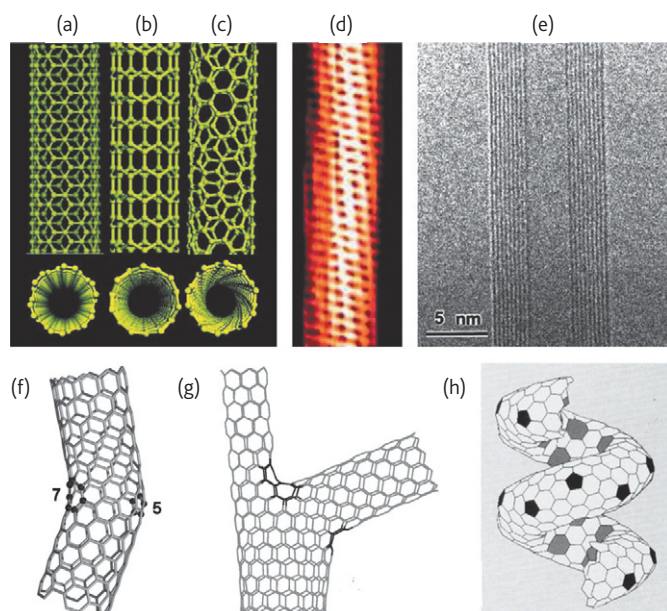


Fig. 1 Schematic illustrations of the structures of (a) armchair, (b) zigzag, and (c) chiral SWNTs. Projectors normal to the tube axis and perspective views along the tube axis are on the top and bottom, respectively. (d) SPM picture of a 1.3 nm diameter chiral SWNT.<sup>3</sup> (e) TEM image of a MWNT containing a concentrically nested array of nine SWNTs. (f) illustration of the carbon-bone network of a kink junction constructed between an 'armchair' tube and a 'zigzag' tube, where 5 denotes a pentagon, 7 denotes a heptagon, and the atoms in the pentagon and heptagon are highlighted by dark balls. (g) Structural model of SWNT asymmetric, zig-zag Y junction.  $n$ -H rings highlighted in dark. (h) Scheme of the helically coiled SWNT (Helix C360) that have the lowest cohesive energy per atom. (Parts (a), (b), (c), and (e) are adapted and reprinted with permission from<sup>2</sup>. © 2002 AAAS. Part (d) is adapted and reprinted with permission from<sup>3</sup>. © 1998 Nature Publishing Group. Part (f) is adapted and reprinted with permission from<sup>11</sup>. © 1999 Nature Publishing Group. Part (g) is adapted and reprinted with permission from<sup>12</sup>. © 2001 AIP. Part (h) is adapted and reprinted with permission from<sup>5</sup>. © 1993 APS.)

tubule segment<sup>16</sup>. To date, a large variety of tubule morphologies have been observed and synthesized. They can be classified into the following categories: straight, waved, coiled, regularly bent, branched, and beaded.

### Straight carbon nanotubes

A variety of techniques have been developed to produce CNTs. MWNTs were synthesized and observed a few decades ago<sup>17,18</sup>. In 1993, Iijima *et al.*<sup>19</sup> and Bethune *et al.*<sup>20</sup> independently reported the synthesis of SWNTs. Primary synthesis methods for single-wall and multi-walled CNTs include arc discharge<sup>4,19-21</sup>, laser ablation<sup>22,23</sup>, gas-phase catalytic growth from carbon monoxide<sup>24</sup>, and chemical vapor deposition (CVD) from hydrocarbons<sup>25</sup>. Synthesis methods such as arc discharge, laser ablation, and certain types of CVD with floating catalysts produce nonaligned, entangled ropes of nanotubes. The diameter of a CNT is in the order of nanometers, while its length can be up to several millimeters. Long CNTs usually can remain straight when they are in oriented structures.

Vertical alignment conventionally means that CNTs are oriented perpendicular to the substrate. A variety of methods for the production

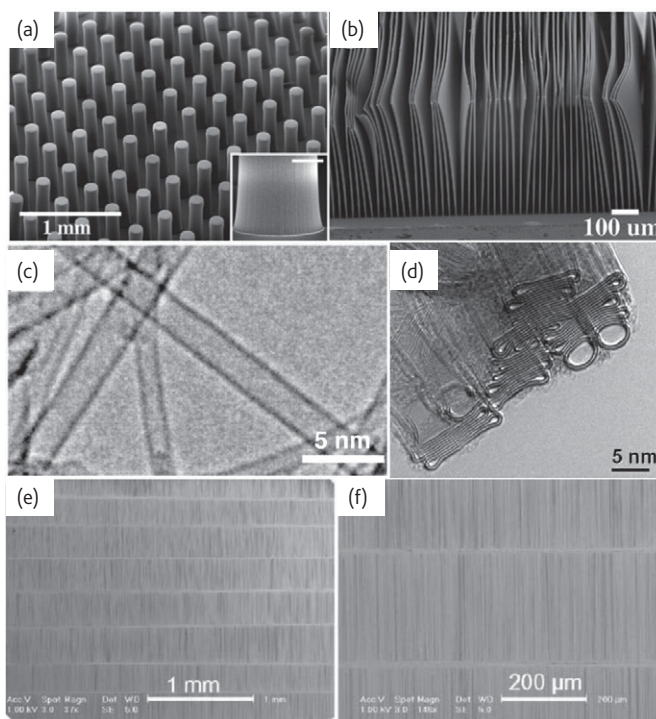


Fig. 2 (a) Scanning electron microscope (SEM) image of SWNT cylindrical pillars with 150  $\mu\text{m}$  radius, 250  $\mu\text{m}$  pitch, and  $\sim 1$  mm height. Insert, SEM image of a root of a pillar. (b) SEM images of SWNT sheets 10  $\mu\text{m}$  thick. (c) High-resolution TEM image of the SWNTs. (d) TEM image of a bundle consists of collapsed single-wall, double-wall, and triple-wall nanotubes with big diameters. Note both the "dog-bone" cross section of these tubes and the non-collapsed tubes at the edge of the bundle. (e) and (f) SEM images of arrays of almost exclusively semiconducting SWNTs at different magnifications. The bright and parallel horizontal lines visible in the images are catalyst lines. (Parts (a), (b), and (c) are adapted and reprinted with permission from<sup>28</sup>. © 2004 AAAS. Part (d) is adapted and reprinted with permission from<sup>29</sup>. © 2007 WILEY. Parts (e) and (f) are adapted and reprinted with permission from<sup>48</sup>. © 2009 ACS)

of aligned arrays in catalytic CVD has been demonstrated and is reviewed<sup>26</sup>. There are two major breakthroughs in the synthesis of CNT arrays. In 1999, Fan *et al.*<sup>27</sup> used porous silicon substrates with a catalyst patterned by electron-beam evaporation through shadow masks to produce MWNT blocks that grew perpendicular to the substrate. Five years later, Hata *et al.*<sup>28</sup> first successfully produced millimeter high SWNT arrays using water assisted CVD (Fig. 2a-c). It is observed that the SWNTs or double-wall CNTs easily collapse, generating stacks of parallel graphene layers, when their diameters are larger than  $\sim 5$  nm (Fig. 2d)<sup>29</sup>.

Horizontally well-aligned CNT arrays on suitable substrates are highly desired for SWNT device applications, such as field effect transistors<sup>30</sup>, sensors<sup>31</sup>, light emitters<sup>32</sup>, logic circuits<sup>33</sup>, and other systems. The most attractive approach is direct growth<sup>34</sup> by CVD with an external force. The external forces can originate from an electric field<sup>35</sup>, the gas flow<sup>36,37</sup>, or interactions with the substrate surface<sup>38-44</sup>. Among them, the surface-guided growth on single crystal substrates such as sapphire<sup>38</sup> or quartz<sup>39-41</sup> provides high density and perfect

alignment<sup>45</sup>. It shows that uniform nanotube arrays fabricated on single crystal substrates can be used directly as a thin film for making a large amount of devices<sup>45-47</sup>. It has been demonstrated that a large variety of metals (including Fe, Co, Ni, Cu, Pt, Pd, Mn, Mo, Cr, Sn, Au, Mg, and Al) can catalyze SWNTs growth. They all show horizontally aligned lattice growth of CNTs on quartz substrates under the same growth conditions<sup>43</sup>. A hypothesis is proposed in which the precipitated carbon shell on the outer surface of the metal catalysts guides the alignment along the crystal lattice but not the catalysts themselves. Recently, high-density arrays of horizontally aligned semiconducting SWNTs were successfully grown on ST-cut single crystal quartz substrates<sup>48</sup>. As shown in Figs. 2e-f, the degree of alignment and linearity in the SWNT arrays is extremely high.

### Waved carbon nanotubes

A single nanotube naturally curves (in bending status) during growth if no external forces exist. In principle, the CNT bending (kinks) can originate from a pentagon-heptagon topological defect pair as

illustrated in Fig. 1f or a local mechanical deformation in a uniform nanotube. A nanotube elastically deforms under a small bending stress, and buckles if the local curvature exceeds a critical value<sup>49,50</sup>. During growth, the bending stress can come from the nanotube's own weight, interaction with neighbor nanotubes, or limited growing space.

A group of CNTs can form a randomly oriented CNT mat or super-aligned CNT arrays, depending on the density of catalyst and their activities under the same synthesis conditions. Figs. 3a-b show a MWNT thin sheets array. These ~100 μm height sheets were grown from 0.2 μm wide and 40 μm long catalyst thin films patterned by e-beam lithography. There were no external forces during sheets growth. The sheets bend when their height is over a certain level. The bending directions and angles depend on each sheet's morphologies. The nanotubes within each sheet confine the nearest neighbors and attract the outermost nanotubes to their neighbors via van der Waals force, thereby producing oriented growth. However, the CNTs in such thin sheets present random curvatures and are tangled (Fig. 3c) because of the weak confinement in thickness direction. As the thickness of the

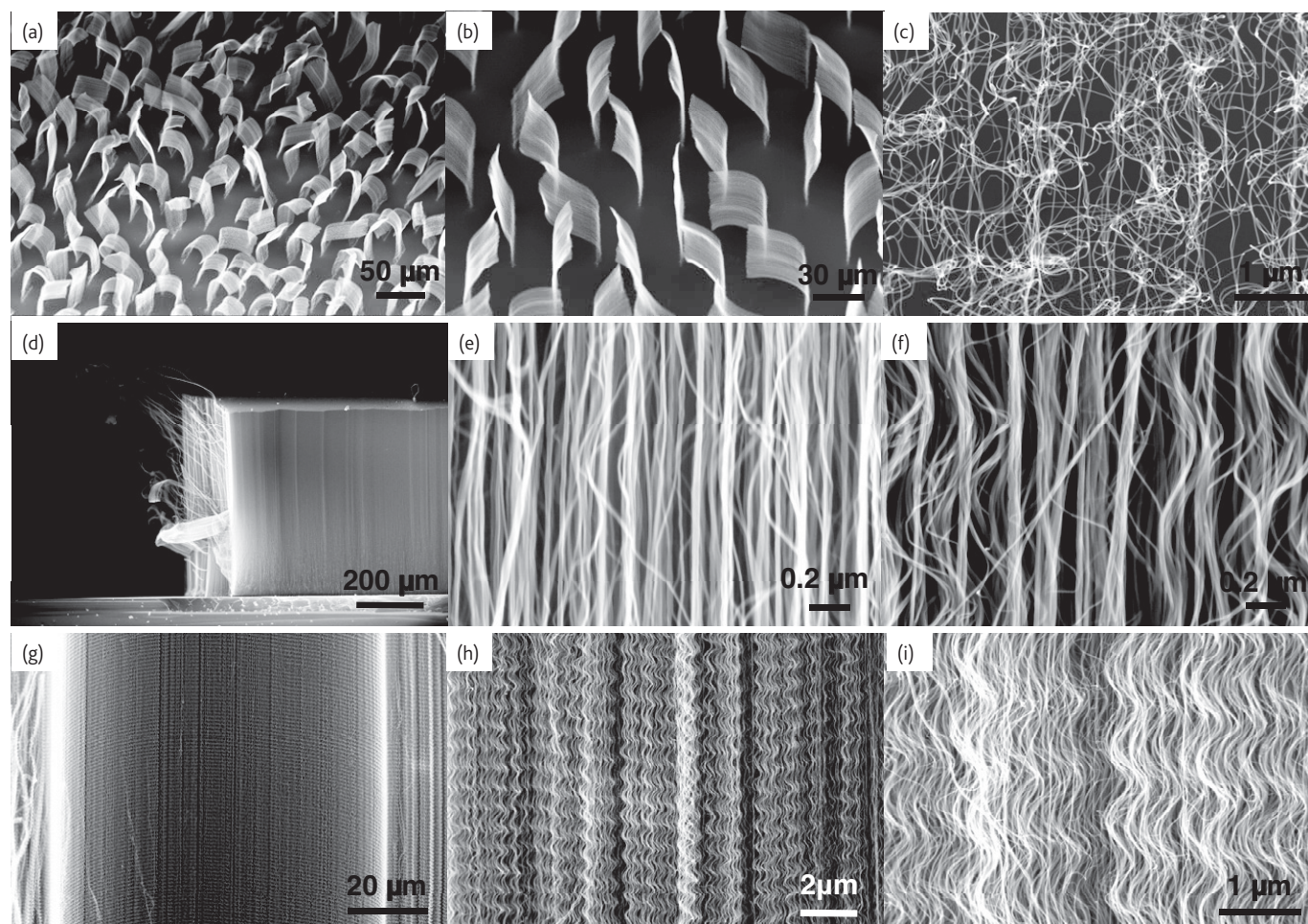


Fig. 3 (a) and (b) SEM images of CNT thin sheets array. The ~100 μm height sheets were grown from 0.2 μm wide and 40 μm long catalyst thin films. (c) CNTs in the thin sheet. (d) and (e) super-aligned MWNT array. (f) Straight and waved MWNTs in an array. (g) to (i) SEM images of a MWNT array with wavy structure at different magnifications.

sheet increases, the alignment of the CNTs could be improved due to the crowding effect. Fig. 3d shows a block of MWNT array, in which nanotubes are super-aligned (Fig. 3e).

Fig. 3g-i show a special CNT array, in which more than 80% of the CNTs are not straight; they periodically bend within fixed intervals throughout their entire length. As a result of this regular bending, a wavy structure is formed. It is believed that the wavy structure is formed because there are roughly two groups of catalysts uniformly distributed on the substrate: one is more active and results in higher CNT growth rate than the other. Due to van der Waals force, which sticks nanotubes together whenever they touch, the growth rate of the array is limited by the nanotubes with the relatively slow growth rate when catalysts stay on the surface of the substrate. The nanotubes with higher growth rate are forced to bend periodically. The period of the wavy is related with the ratio of growth rates of these two groups. When the distribution of the catalyst activity is broad but the density is high, the array will have the morphology as shown in Fig. 3f. The straight CNTs bundled while the waved CNTs switch between different bundles. Such structure is believed important for assembling CNT sheets or yarns by drawing CNTs directly from the array<sup>51-53</sup>.

### Coiled carbon nanotubes

Coiled CNTs were predicted in the early 1990s<sup>6,54</sup>. These CNTs are created when paired pentagon-heptagon atomic rings arrange themselves periodically within the hexagonal carbon network<sup>55</sup>. Theoretical calculation also predicted that various forms of helically coiled structures are possible and those structures are energetically and thermodynamically stable<sup>7</sup>. Helical structures of carbon have been observed as early as 1950s<sup>56</sup>. Coiled CNTs were observed experimentally in 1994<sup>16</sup>.

Fig. 4a shows coiled CNTs grown on iron-coated indium tin oxide substrate by catalytic CVD<sup>57</sup>. More than 95% of CNTs are in helical structures. The coils have various diameters and pitches. They grow out of the substrate and maintain their self-organization well during growth. It is interesting to note that each coil grows with its own pitch and diameter. Later investigations evidenced that indium and tin play an important role in the formation of coiled CNTs<sup>58,59</sup>. The double and triple helices are often observed too (Fig. 4c)<sup>57,60</sup>. So far, synthesized coiled CNTs are MWNTs with more or less incomplete crystalline structures. Coiled SWNTs have not been recorded.

Several mechanisms were hypothesized for the formation of coiled CNTs. Regular insertion of pentagon-heptagon pairs at the junction, as predicted theoretically, is for CNTs without other crystallographic defects. The model of localized stresses and anisotropic rates of carbon deposition<sup>57,61,62</sup> on catalyst particles is most widely accepted. Recently, a thermodynamic model<sup>63</sup> was proposed for providing a comprehensive explanation, where helix/coil formation is explained on the basis of the interactions between specific catalyst particles and growing nanostructures. Coiled CNTs can be produced at high yield by catalytic CVD<sup>16,57,61,64-66</sup>.

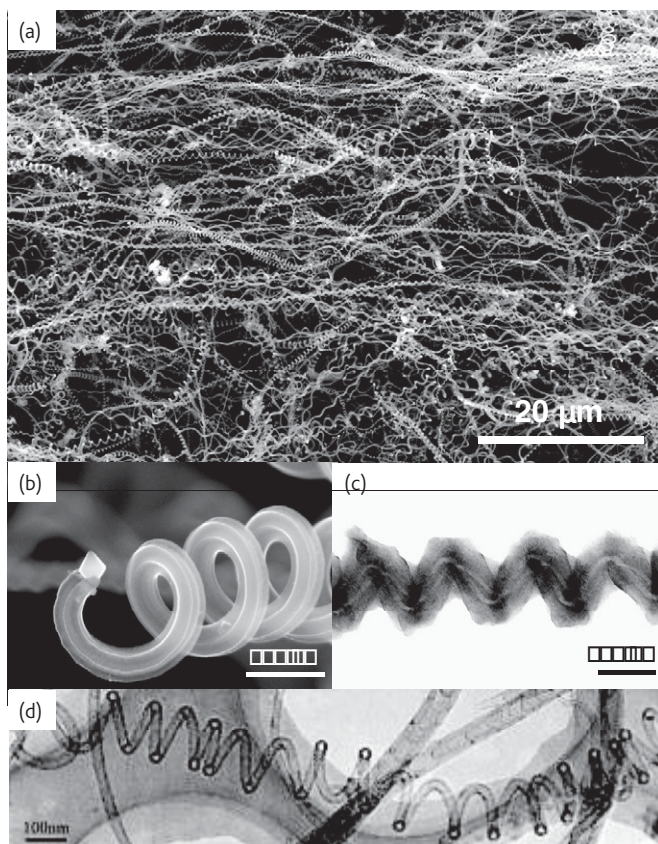


Fig. 4 Coiled CNTs. (a) SEM image of large amount of helically coiled CNTs<sup>61</sup>. Each coil grows with its own diameter and pitch. (b) The tip of a coil. (c) TEM image of a coil formed by two tubules with the same pitch but different diameters and a slight shift in phase. (d) TEM image of typical coiled CNTs. (Part (d) is adapted and reprinted with permission from<sup>62</sup>. © 2003 AIP.)

Coiled CNTs are attracting because their peculiar morphology enables them to be used as high-performance electromagnetic wave absorbers, sensors, resonators, nanoscale mechanical springs, electrical inductors, and generators of magnetic beams. For applications, it would be desirable to have control over the coil morphology and geometry (diameter, pitch, length, and turning direction).

### Regularly bent carbon nanotubes

Regularly bent CNTs are proposed for applications including mechanical nanospring devices, high-resolution AFM tips, and nanocircuit interconnections in device. It is known that CNTs can be aligned during growth with an external force originated from an electric field<sup>35</sup>, the gas flow<sup>36,37</sup>, or interactions with the substrate surface<sup>38,67</sup>. Properly combining those external forces is a way to make regularly bent CNTs. Fig. 5a shows a zigzag shaped SWNT, which is formed due to the SWNT-substrate lattice interaction and the gas flow<sup>67</sup>.

Arrays of CNTs with zigzag morphology are shown in Fig. 5b. The zigzag morphologies consist of 2-4 very sharp and alternating  $\sim 90^\circ$  bends. They were grown using a dc plasma enhanced CVD process<sup>68</sup>. The bending of the CNTs during growth was caused by changing the

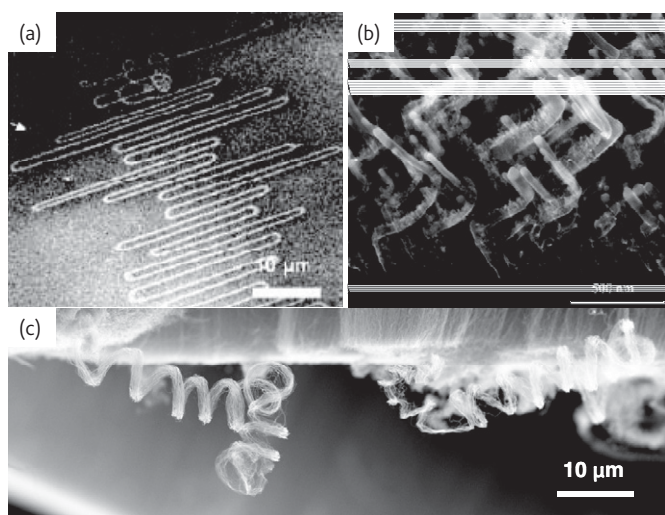


Fig. 5 (a) SEM image of a self-organized SWNT serpentine formed due to the combined alignment effects from the quartz substrate and gas flow. (b) Array of CNTs grown with zigzag morphology using a three-stage growth process. Sample tilted 45° for SEM analysis. (c) A small group of MWNTs forms a coil-like structure by self assembly. (Part (a) is adapted and reprinted with permission from<sup>67</sup>. © 2007 ACS. Part (b) is adapted and reprinted with permission from<sup>68</sup>. © 2004 ACS.)

direction of the electric field lines in the growth region of the sample. It is anticipated that such a sharp bend in a nanotube is likely to contain many defects, not only pentagon and heptagon defects. To utilize CNTs as interconnectors and other device components, the ability to control their growth morphology is desired, especially if SWNTs or small diameter MWNTs can also be made to respond to electrical field manipulations and bend in a similar fashion.

Self assembly can form some novel structures. Fig. 5c records a small group of CNTs that bundle together, regularly bend during growth, and result in a coil like structures.

### Branched carbon nanotubes

The first structural models<sup>69,70</sup> for CNT Y-junctions are based on the insertion of non-hexagonal rings in the hexagonal network in the region where the three branches of the Y are joined together. All the subsequent structural models<sup>71-73</sup> follow the same construction principle of conserving the  $sp^2$  hybridization of the carbon network, differing only in the kind, number, and placement of the non-hexagonal rings. These variations make possible the constructions of various symmetric and asymmetric model junctions<sup>74,75</sup> and various angles from Y to T shapes<sup>12,71</sup>. Since the electrical properties of CNTs are dependent on the tube structure (chirality and diameter), various combinations of metallic and semiconducting tubes can be built to form CNT junctions as building parts for nanoscale integrated circuits<sup>76,77</sup>.

Branched nanotubes with T, Y, L, and more complex junctions were initially observed in arc-discharge produced nanotubes<sup>78</sup>. The first synthesis was reported in 1999 by pyrolysis of acetylene in Y-shaped templates<sup>79</sup>. Since then, most work has focused on catalytic

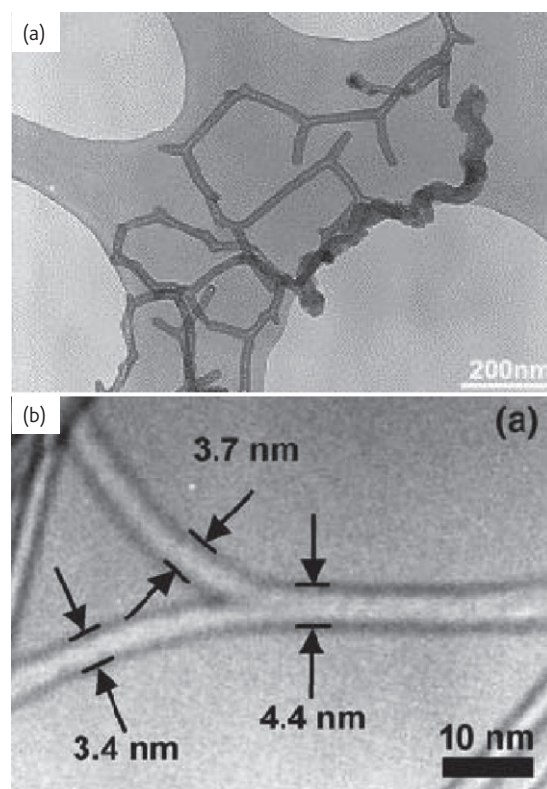


Fig. 6 (a) SEM image of branched CNTs. (b) TEM images of a typical Y-junction SWNT. (Part (a) is adapted and reprinted with permission from<sup>88</sup>. © 2005 Elsevier. Part (b) is adapted and reprinted with permission from<sup>90</sup>. © 2005 Elsevier.)

CVD<sup>80-88</sup>. Several processes and mechanisms were presented. A single-particle process<sup>83,84,88</sup> attributed the formation of branched CNTs to fluctuation in temperature, gas flow, or carbon source feeding, which could change the distribution of carbon atoms on the catalyst particles and alter the growth direction to form a multi-stem CNT<sup>88</sup> (Fig. 6a). A splitting process<sup>85,86</sup> posited that the liquid-phase metal-carbon solution encapsulated in a CNT could split into smaller particles and lead to the growth of branched CNTs. A merging process<sup>81,87</sup> proposed that catalyst particles encapsulated in two neighboring CNTs could weld together to form a larger catalyst particle which then catalyzes the growth of a third CNT branch. Catalyst particles attached to the CNT sidewall could also result in branched growth, and the doping metals (Ti<sup>89</sup> or Mo<sup>90</sup>) play important roles in the attachment process. A multibranching CNT structure synthesized by dc plasma enhanced CVD has been reported<sup>91</sup>. The structure consists of aligned CNTs which have branches of smaller diameters growing aligned along a direction perpendicular to the original CNT. Most of these processes generate branched MWNTs, some of them are with poor crystallographic structures.

Branched SWNTs are believed to have a profound impact on next-generation electronic devices since they have a potential to be used in nano-electronic devices as nano-diode, nano-transistor, and nano-

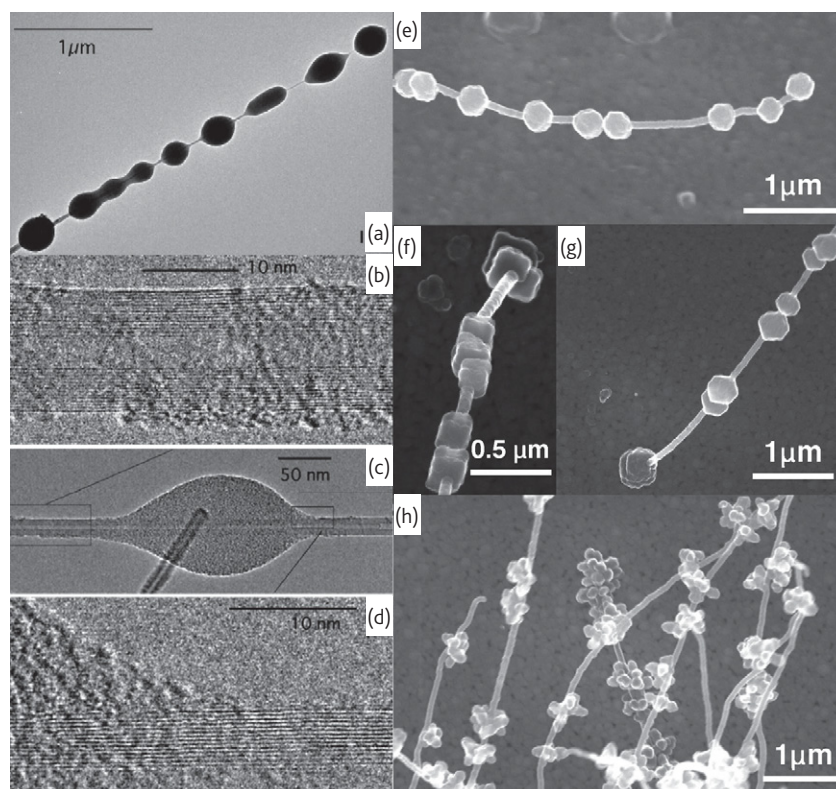


Fig. 7 Various beaded CNTs. (a) TEM image of a MWNT with many beads. (c) TEM image of a small, elongated bead on a 15-layer MWNT. (b) and (d) High-resolution TEM images of the furthest extent of the meniscus on the left side of the bead and the bead meniscus to the right. (e-h) SEM images of beads in different shapes<sup>95</sup>: sphere (e), cubic (f), polyhedral (g), and bloom-shaped beads (h). (Parts (a) to (d) are adapted and reprinted with permission from<sup>96</sup>. © 2005 AAAS.)

interconnect. The electronic properties of SWNT Y-junctions have been modeled theoretically<sup>92</sup> and measured experimentally<sup>93,94</sup>. They show great potential as elements in simple nanoelectronic devices. Y-junction SWNTs have been successfully synthesized using controlled catalysts by thermal CVD<sup>90</sup>, where Mo-doped Fe nanoparticles supported by aluminum oxide particles are used as catalysts. It is found that distribution of Mo-doped Fe particles plays an important role in Y-junction formation. Fig. 6b shows a typical TEM image of SWNT Y-junction with diameters of 2-5 nm.

### Carbon nanotubes with beads

CNTs with beads were observed from different processes<sup>18,95-98</sup>. Beads appear in various patterns and their structures are either amorphous or polycrystalline graphite. The beads form either with<sup>18,95</sup> or after CNT formation<sup>96,97</sup> during synthesis. CNT's crystallographic structures may not be disturbed in some cases.

Fig. 7a shows a MWNT with 100 to 200 nm diameter beads. These beaded nanotubes are occasionally found on the surface of the columns harvested from the interior of the arc deposition<sup>96</sup>. The beads are carbon glass (amorphous phase). They formed on nanotube because carbon coated on the nanotube was a viscous liquid and cooling caused the viscosity to increase to a degree that the beading process stagnated. The nanotube is clearly visible inside the bead (Fig. 7b-d). There is no

evidence for graphitic layering in the bead, nor does the bead distort the nanotube.

The beaded CNTs also formed in relatively low temperature (~700 °C) CVD process<sup>95</sup>. Various shapes, such as spherical, cubic, other polyhedron, and bloom shaped structures, were observed (Fig. 7e-h). The dense packaged beads form thick-stick like structures around the CNT. It is believed that those chaplets are formed during nanotube growth and the shape of the beads is related to catalyst-included seeds<sup>95</sup>.

Beaded CNTs are expected as fillers in composites to enhance the electric conductivity and/or mechanical properties of the matrix materials because the beads on CNTs prevent slipping of the nanotubes in the composite materials.

### Summary

CNTs have various tubule morphologies and appear in different shapes. Each shape has its own special properties and potential applications. CNTs in different shapes will have significant impacts only when they can be produced with uniform properties in large quantities. Precise control of a CNT's morphology at specific positions by synthesis is still challenge. 

### Acknowledgments

This work was supported by the Air Force Research Laboratory.

REFERENCES

- 1 Louie, S. G., *Top. Appl. Phys.* (2001) **80**, 113
- 2 Baughman, R. H., *et al.*, *Science* (2002) **297**, 787
- 3 Wildoer, J. W. G., *et al.*, *Nature* (1998) **391**, 59
- 4 Iijima, S., *Nature* (1991) **354**, 56
- 5 Ihara, S., *et al.*, *Phys. Rev. B* (1993) **47**, 12908
- 6 Dunlap, B. I., *et al.*, *Phys. Rev. B* (1992) **46**, 1933
- 7 Ihara, S., *et al.*, *Phys. Rev. B* (1993) **48**, 5643
- 8 Macky, A. L., *et al.*, *Nature* (1991) **352**, 762
- 9 Scuseria, G. E., *Chem. Phys. Lett.* (1992) **195**, 534
- 10 Chernozatonskii, L. A., *Phys. Lett. A* (1992) **172**, 173
- 11 Yao, Z., *et al.*, *Nature* (1999) **402**, 273
- 12 Andriotis, A. N., *et al.*, *Appl. Phys. Lett.* (2001) **79**, 266
- 13 Dunlap, B. I., *et al.*, *Phys. Rev. B* (1994) **49**, 5643
- 14 Biro, L. P., *et al.*, *Phys. Rev. B* (2002) **66**, 165405
- 15 Lambin, Ph., *Phys. Rev. B* (2003) **67**, 205413
- 16 Amelinckx, S., *et al.*, *Science* (1994) **256**, 635
- 17 Radushkevich, L. V., and Lukyanovich, V. M., *Zurn. Fisc. Chim.* (1952) **26**, 88
- 18 Oberlin, A., *et al.*, *J. Cryst. Growth* (1976) **32**, 335
- 19 Iijima, S., and Ichihashi, T., *Nature* (1993) **363**, 603
- 20 Bethune, D. S., *et al.*, *Nature* (1993) **363**, 605
- 21 Journet, C., *et al.*, *Nature* (1997) **388**, 756
- 22 Rinzler, A. G., *et al.*, *Appl. Phys. A* (1998) **67**, 29
- 23 Guo, T., *et al.*, *Chem. Phys. Lett.* (1995) **243**, 49
- 24 Nikolaev, P., *et al.*, *Chem. Phys. Lett.* (1999) **313**, 91
- 25 Ren, Z. F., *et al.*, *Science* (1998) **282**, 1105
- 26 Huczko, A., *Appl. Phys. A: Mater. Sci. Process* (2002) **74**, 617
- 27 Fan, S. S., *et al.*, *Science* (1999) **283**, 512
- 28 Hata, K., *et al.*, *Science* (2004) **306**, 1362
- 29 Motta, M., *et al.*, *Adv. Mater.* (2007) **19**, 3721
- 30 Tans, S. J., *et al.*, *Nature* (1998) **393**, 49
- 31 Kong, J., *et al.*, *Science* (2000) **287**, 622
- 32 Misewich, J. A., *et al.*, *Science* (2003) **300**, 783
- 33 Bachtold, A., *et al.*, *Science* (2001) **294**, 1317
- 34 Kong, J., *et al.*, *Nature* (1998) **395**, 878
- 35 Ural, A., *et al.*, *Appl. Phys. Lett.* (2002) **81**, 3464
- 36 Huang, S. M., *et al.*, *J. Am. Chem. Soc.* (2003) **125**, 5636
- 37 Zhong, J., *et al.*, *Nano Lett.* (2007) **7**, 2073
- 38 Han, S., *et al.*, *J. Am. Chem. Soc.* (2005) **127**, 5294
- 39 Ismach, A., *et al.*, *Angew. Chem., Int. Ed.* (2004) **43**, 6140
- 40 Kocabas, C., *et al.*, *Small* (2005) **1**, 1110
- 41 Hur, S. H., *et al.*, *J. Appl. Phys.* (2005) **98**, 114302.
- 42 Yoshihara, N., *et al.*, *J. Phys. Chem. C* (2009) **113**, 8030
- 43 Yuan, D. *et al.*, *Nano Lett.* (2008) **8**, 2576
- 44 Zhou, W., *et al.*, *J. Nano Res.* (2008) **1**, 158
- 45 Kang, S. J., *et al.*, *Nat. Nanotechnol.* (2007) **2**, 230
- 46 Ding, L., *et al.*, *J. Am. Chem. Soc.* (2008) **130**, 5428
- 47 Orofeo, C. M., *et al.*, *Appl. Phys. Lett.* (2009) **94**, 053113
- 48 Ding, L., *et al.*, *Nano Lett.*, (2009) **9**, 800
- 49 Iijima, S., *et al.*, *J. Chem. Phys.* (1996) **104**, 2089)
- 50 Yakobson, B. I., *et al.*, *Phys. Rev. Lett.* (1996) **76**, 2511
- 51 Zhang, M., *et al.*, *Science* (2004) **306**, 1358
- 52 Zhang, M., *et al.*, *Science* (2005) **309**, 1215
- 53 Zhang, X., *et al.*, *Adv. Mater.* (2006) **18**, 1505
- 54 Itoh, S., *et al.*, *Phys. Rev. B* (1993) **48**, 8323
- 55 Gao, R. P., *et al.*, *J. Phys. Chem. B* (2000) **104**, 1227
- 56 Davis, W. R., *et al.*, *Nature* (1953) **171**, 756
- 57 Zhang, M., *et al.*, *Jpn. J. Appl. Phys.* (2000) **39**, L1242
- 58 Wang, W., *Adv. Mater.* (2008) **20**, 179
- 59 Pan, L., *et al.*, *J. Appl. Phys.* (2002) **91**, 10058
- 60 Su, C. J., *et al.*, *Phys. Chem. Comm.* (2002) **5**, 34
- 61 Ivanov, V., *et al.*, *Chem. Phys. Lett.* (1994) **223**, 329
- 62 Zhong, D. Y., *et al.*, *Appl. Phys. Lett.* (2003) **83**, 4423
- 63 Bandaru, P. R., *et al.*, *J. Appl. Phys.* (2007) **101**, 094307
- 64 Hou, H., *et al.*, *Chem. Mater.* (2003) **15**, 3170
- 65 Lu, M., *et al.*, *J. Phys. Chem. B* (2004) **108**, 6186
- 66 Wang, J. N., *et al.*, *Cryst. Growth Des.* (2008) **8**, 1741
- 67 Kocabas, C., *et al.*, *J. Phys. Chem. C* (2007) **111**, 17879
- 68 AuBuchon, J. F., *et al.*, *Nano Lett.*, (2004) **4**, 1781
- 69 Scuseria, G. E., *Chem. Phys. Lett.* (1992) **195**, 534.
- 70 Chernozatonskii, L. A., *Phys. Lett. A* (1992) **172**, 173
- 71 Menon, M., and Srivastava, D., *Phys. Rev. Lett.* (1997) **79**, 4453.
- 72 Treboux, G., *et al.*, *Chem. Phys. Lett.* (1999) **306**, 402.
- 73 Meunier, V., *et al.*, *Appl. Phys. Lett.* (2002) **81**, 5234
- 74 Andriotis, A. N., *et al.*, *Phys. Rev. B* (2002) **65**, 165416
- 75 Xue, B., *et al.*, *Comput. Mater. Sci.* (2008) **43**, 531
- 76 Popov, V. N., *Mater. Sci. Eng. R* (2004) **43**, 61
- 77 Dunlap, B. I., *Phys. Rev. B* (1992) **46**, 1933
- 78 Zhou, D., and Seraphin, S., *Chem. Phys. Lett.* (1995) **238**, 286
- 79 Li, J., *et al.*, *Nature* (1999) **402**, 253
- 80 Satishkumar, B. C., *et al.*, *Appl. Phys. Lett.* (2000) **77**, 2530
- 81 Wei, D. C., *et al.*, *Nano Lett.*, (2006) **6**, 186
- 82 Luo, C., *et al.*, *Carbon* (2008) **46**, 440
- 83 Su, L. F., *et al.*, *Chem. Vapor Depos.* (2005) **11**, 351
- 84 Tao, X. Y., *et al.*, *Chem. Phys. Lett.* (2005) **409**, 89
- 85 Huang, S. M., *et al.*, *Physica B* (2002) **323**, 336
- 86 Ding, D. Y., *et al.*, *Appl. Phys. A* (2005) **81**, 805
- 87 Lee, T. J., *et al.*, *Carbon* (2005) **43**, 1341
- 88 Heyning, O. T., *Chem. Phys. Lett.* (2005) **409**, 43
- 89 Gothard, N., *et al.*, *Nano Lett.* (2004) **4**, 213
- 90 Choi, Y. C., and Choi, W., *Carbon* (2005) **43**, 2737
- 91 AuBuchon, J. F., *et al.*, *Nano Lett.* (2006) **6**, 324
- 92 Treboux, G. J., *Phys. Chem. B* (1999) **103**, 10378
- 93 Bandaru, P. R., *J. Mater. Sci.* (2007) **42**, 1809
- 94 Papadopoulos, C., *et al.*, *Phys. Rev. Lett.* (2000) **85**, 3476
- 95 Nakayama, Y., and Zhang, M., *Jpn. J. Appl. Phys.* (2001) **40**, L492
- 96 de Heer, W. A., *et al.*, *Science* (2005) **307**, 907
- 97 Monthieux, M., *et al.*, *Carbon* (2006) **44**, 3183
- 98 Ting, J. M., and Lan, J. B. C., *Appl. Phys. Lett.* (1999) **75**, 3309